

## Optical Photometry of GRB 021004: The First Month<sup>1</sup>

Stephen T. Holland<sup>2</sup>, Michael Weidinger<sup>3</sup>, Johan P. U. Fynbo<sup>3</sup>, Javier Gorosabel<sup>4,5</sup>, Jens Hjorth<sup>6</sup>,  
Kristian Pedersen<sup>6</sup>, Javier Méndez Alvarez<sup>11,12</sup>, Thomas Augusteijn<sup>7</sup>, J. M. Castro Cerón<sup>8</sup>,  
Alberto Castro-Tirado<sup>5</sup>, Håkon Dahle<sup>9</sup>, M. P. Egholm<sup>3,7</sup>, Páll Jakobsson<sup>6</sup>, Brian L. Jensen<sup>6</sup>,  
Andrew Levan<sup>10</sup>, Palle Møller<sup>13</sup>, Holger Pedersen<sup>6</sup>, Tapio Pursimo<sup>7</sup>, Pilar Ruiz-Lapuente<sup>12</sup>, &  
Bjarne Thomsen<sup>3</sup>

## ABSTRACT

---

<sup>2</sup>Department of Physics, University of Notre Dame, Notre Dame, IN 46556–5670, U.S.A.

`sholland@nd.edu`

<sup>3</sup>Department of Physics & Astronomy, University of Aarhus, Ny Munkegade, DK–8000 Århus C, Denmark

`michaelw@phys.au.dk`, `jfynbo@phys.au.dk`, `mpe@not.iac.es`, `bt@phys.au.dk`

<sup>4</sup>Laboratorio de Astrofísica Espacial y Física Fundamental (INTA), Apartado de Correos, 50.727, E–28.080 Madrid, Spain

`jgu@laeff.esa.es`

<sup>5</sup>Instituto de Astrofísica de Andalucía (IAA-CSIC), Apartado de Correos, 3.004, E–18.700 Granada, Spain

`jgu@iaa.es`, `ajct@iaa.es`

<sup>6</sup>Astronomical Observatory, University of Copenhagen, Juliane Maries Vej 30, DK–2100 Copenhagen Ø, Denmark

`jens@astro.ku.dk`, `kp@astro.ku.dk`, `pallja@astro.ku.dk`, `brian_j@astro.ku.dk`,  
`holger@astro.ku.dk`

<sup>7</sup>Nordic Optical Telescope, Apartado de Correos, 474, E–38.700 Santa Cruz de la Palma (Tenerife), Spain

`tau@not.iac.es`, `tpursimo@not.iac.es`

<sup>8</sup>Real Instituto y Observatorio de la Armada, Sección de Astronomía, E–11.110 San Fernando–Naval (Cádiz), Spain

`josemari@alumni.nd.ed`

<sup>9</sup>NORDITA, Blegdamsvej 17, DK–2100 Copenhagen Ø, Denmark

`dahle@nordita.dk`

<sup>10</sup>Department of Physics and Astronomy, University of Leicester, University Road, Leicester, LE1 7RH, UK

`anl@star.le.ac.uk`

<sup>11</sup>Isaac Newton Group of Telescopes, Apartado de Correos 321, E–38.700 Santa Cruz de la Palma, Spain

`jma@ing.iac.es`

<sup>12</sup>Departamento de Astronomía y Meteorología, Universidad de Barcelona, Martí i Franquès 1, E–08.028 Barcelona, Spain

`pilar@mizar.am.ub.es`

<sup>13</sup>European Southern Observatory, Karl–Schwarzschild–Straße 2, D–85748 Garching bei München, Germany

`pmoller@eso.org`

We present  $UBVR_CI_C$  photometry of the optical afterglow of the gamma-ray burst GRB 021004 taken at the Nordic Optical Telescope between approximately eight hours and 30 days after the burst. This data is combined with an analysis of the 87 ksec *Chandra X-ray* observations of GRB 021004 taken at a mean epoch of 33 hours after the burst to investigate the nature of this GRB. We find an intrinsic spectral slope at optical wavelengths of  $\beta_{UH} = 0.39 \pm 0.12$  and an  $X$ -ray slope of  $\beta_X = 0.94 \pm 0.03$ . There is no evidence for color evolution between 8.5 hours and 5.5 days after the burst. The optical decay becomes steeper approximately five days after the burst. This appears to be a gradual break due to the onset of sideways expansion in a collimated outflow. Our data suggest that the extra-galactic extinction along the line of sight to the burst is between  $A_V \approx 0.3$  and  $A_V \approx 0.5$  and has an extinction law similar to that of the Small Magellanic Cloud. The optical and  $X$ -ray data are consistent with a relativistic fireball with the shocked electrons being in the slow cooling regime and having an electron index of  $p = 1.9 \pm 0.1$ . The burst occurred in an ambient medium that is homogeneous on scales larger than approximately  $10^{18}$  cm but inhomogeneous on smaller scales. The mean particle density is similar to what is seen for other bursts ( $0.1 \lesssim n \lesssim 100 \text{ cm}^{-3}$ ). Our results support the idea that the brightening seen approximately 0.1 days was due to interaction with a clumpy ambient medium within  $10^{17}$ – $10^{18}$  cm of the progenitor. The agreement between the predicted optical decay and that observed approximately ten minutes after the burst suggests that the physical mechanism controlling the observed flux at  $t \approx 10$  minutes is the same as the one operating at  $t > 0.5$  days.

*Subject headings:* gamma rays: bursts

## 1. Introduction

The gamma-ray burst (GRB) GRB 021004 was detected in the constellation Pisces by the FREGATE, WXM, and SXC instruments on board the *High Energy Transient Explorer II (HETE-II)* satellite at 12:06:13.57 UT on 2002 Oct. 4 (Shirasaki et al. 2002). The burst had a duration of approximately 100 s and consisted of two peaks separated by approximately 25 s. Each peak had a fast rise and exponential decay profile and a power-law spectrum with a slope of 1.64 (Lamb et al. 2002). The FREGATE instrument on *HETE-II* measured a fluence of  $1.3 \times 10^{-6}$  erg  $\text{cm}^{-2}$  between 50 and 300 keV and  $3.2 \times 10^{-6}$  erg  $\text{cm}^{-2}$  between 7 and 400 keV. The WXM fluence (2–25 keV) is

---

<sup>1</sup>Based on observations taken with the Nordic Optical Telescope (NOT), operated on the island of Santa Miguel de la Palma jointly by Denmark, Finland, Iceland, Norway, and Sweden, in the Spanish Observatorio del Roque de los Muchachos of the Instituto de Astrofísica de Canarias, and on observations taken with the *Chandra X-Ray* Observatory.

$7.5 \times 10^{-7}$  erg cm $^{-2}$  (Lamb et al. 2002). Therefore, GRB 021004 was an X-ray rich burst and fits into the long-soft class of bursts (Kouveliotou et al. 1993).

The redshift of the burst was initially constrained to be  $z \geq 1.60$  based on the detection of a Mg II absorption system in the spectrum of the afterglow (Fox et al. 2002). Chernock & Filippenko (2002) found absorption and emission due to Ly $\alpha$  at  $z = 2.33$ . Møller et al. (2002) report on five absorption systems and confirm the presence of the Ly $\alpha$  emission line, from which they derive a host galaxy redshift of  $z = 2.3351$ . The GRB absorption system shows strong similarities with associated QSO absorbers, i.e., an outflow velocity of several 1000 km s $^{-1}$ , high ionization, and line-locking (Salamanca et al. 2002; Savaglio et al. 2002; Møller et al. 2002).

Torii et al. (2002) observed the location of the GRB 3.5 minutes after the burst with the RIKEN automated telescope and found an upper limit for the unfiltered magnitude of 13.6. The optical afterglow (OA) was identified 9.45 minutes after the *HETE-II* trigger by the 48-inch Oschin/NEAT robotic telescope (Fox 2002). The rapid identification allowed for near-continuous monitoring of this burst’s OA. It quickly became apparent that the OA was not following a simple power-law decay but had rebrightened approximately 0.1 days after the burst. Further observations suggested that there were rapid variation in the optical decay (Winn et al. 2002) similar to those seen in GRB 011211 (Holland et al. 2002; Jakobsson et al. 2003), and larger deviations from a power law decay on scales of hours to a day (Winn et al. 2002; Sahu et al. 2002).

The large variations in GRB 021004’s optical decay are unusual, but not unheard of in GRB afterglows. GRB 970508 was the second GRB for which an OA was identified. This OA had a constant luminosity for approximately one day after the burst then brightened by a factor of approximately six before taking on the familiar power-law decay (Castro-Tirado et al. 1998; Pedersen et al. 1998). Panaitescu et al. (1998) showed that this behavior could be explained if there is an additional injection of energy into the external shock at later times. This additional energy could come from a shell of ejecta moving more slowly than the main body of ejecta impacting on the external medium. GRB 000301C also exhibited significant deviations from a broken power-law decay for several days after the burst. Garnavich et al. (2000) found that these deviations were consistent with the OA being microlensed. Holland et al. (2002) and Jakobsson et al. (2003) observed rapid variations in the optical decay of GRB 011211 which Holland et al. (2002) interpret as being due to small-scale density fluctuations in the ambient medium within 0.1 pc of the progenitor. As rapid responses to GRBs become more common optical observations will be able to probe the first few hours of more GRBs and allow observations of the prompt emission. This will provide a window into the physics of the early OA. In this paper we present a self-consistent set of optical observations of GRB 021004 starting approximately 8.5 hours after the burst and covering the first month. We use this data to constrain the physics of the relativistic fireball and probe the ambient medium around the progenitor.

In this paper we adopt a cosmology with a Hubble parameter of  $H_0 = 65$  km s $^{-1}$  Mpc $^{-1}$ , a matter density of  $\Omega_m = 0.3$ , and a cosmological constant of  $\Omega_\Lambda = 0.7$ . For this cosmology a

redshift of  $z = 2.3351$  corresponds to a luminosity distance of 20.22 Gpc and a distance modulus of 46.53. One arcsecond corresponds to 29.39 comoving kpc, or 8.81 proper kpc. The lookback time is 11.56 Gyr.

## 2. The Data

### 2.1. Optical Photometry

The OA for GRB 021004 is located at R.A. = 00:26:54.69, Dec. = +18:55:41.3 (J2000) (Fox 2002), which corresponds to Galactic coordinates of  $(b^{\text{II}}, l^{\text{II}}) = (-43^{\circ}56'16'', 114^{\circ}9'17'')$ . The reddening maps of Schlegel et al. (1998) give a Galactic reddening of  $E_{B-V} = 0.060 \pm 0.020$  mag in this direction. The corresponding Galactic extinctions are  $A_U = 0.325$ ,  $A_B = 0.258$ ,  $A_V = 0.195$ ,  $A_{RC} = 0.160$ ,  $A_{IC} = 0.116$ , and  $A_H = 0.034$ .

We obtained  $UBVR_CI_C$  images of the field containing GRB 021004 using the Andalucía Faint Object Spectrograph and Camera (ALFOSC) and the Mosaic Camera (MOSCA) on the 2.56-m Nordic Optical Telescope (NOT) at La Palma between 2002 Oct. 4 and 2002 Nov. 4. The ALFOSC detector is a  $2048 \times 2048$  pixel thinned Loral CCD with a pixel scale of  $0''.189$ . The instrumental gain was  $1.0 \text{ e}^-/\text{ADU}$  and the read-out noise was  $6 \text{ e}^-/\text{pixel}$ . The MOSCA detector is a  $2 \times 2$  mosaic CCD camera containing four flash-gated Loral-Lesser thinned  $2048 \times 2048$  CCDs. The pixel size is  $15 \mu\text{m}$  and the pixel scale is  $0''.11$ . The instrumental gain is  $1.24 \text{ e}^-/\text{ADU}$  and the read-out noise is  $8.5 \text{ e}^-/\text{pixel}$ . The data from Oct. 19 and Nov. 4 were obtained using MOSCA. All other data were obtained using ALFOSC. Fig. 1 shows the field of GRB 021004.

The data were preprocessed using standard techniques for bias and flat-field corrections. Photometry was performed using DAOPHOT II (Stetson 1987; Stetson & Harris 1988) and calibrated using seven secondary standard stars from the catalogue of Henden (2002) (see Table 1). The magnitude of the OA at each epoch was determined as the weighted average over the OA magnitudes computed relative to each of the secondary standard stars. The weights for each point were the quadratic sum of the DAOPHOT II error and the photometric error for each standard star. The corresponding error in the OA at each epoch was computed as the dispersion of the OA magnitude calculated relative to each of the secondary standards. The log of the observations and the photometry of the OA is presented in Table 2. In some images stars B and F were saturated and were not used for calibration. Henden (2002) did not detect stars C and D in the  $U$ -band, so we could not use them to calibrate our  $U$ -band photometry. The color terms in the calibrations were smaller than 5% and did not improve the quality of the calibrations. Therefore no color corrections were applied to the photometry.

## 2.2. X-Ray Data

*Chandra* High-Energy Transmission Grating data were obtained between 2002 Oct. 5.37 and 2002 Oct. 6.38 (Sako & Harrison 2002). We analyzed the zero'th and first order spectra adopting standard screening criteria for *Chandra* data. In order to constrain the spectral index in the X-ray band, and to look into any dependence on absorption, we made two joint zero'th and first order fits to the data. First, a power-law model was fit to the data in the 2–10 keV band. Second, the data in the full-well calibrated spectral range 0.4–10 keV was fit with an intrinsic power-law model with absorption by Galactic hydrogen. The column density was fixed at  $1.23 \times 10^{20} \text{ cm}^{-2}$  (Dickey & Lockman 1990) while the absorbing column at the redshift of GRB 021004 was left as a free parameter. The *Chandra* data and our fits are shown in Fig. 2.

A pure power law is an excellent fit ( $\chi^2 = 47.8$  for 74 degrees of freedom (DOF)) to the data in the 2–10 keV band with a best fit spectral index of  $\beta_X = 1.03 \pm 0.06$ . A lower, but consistent, spectral index ( $\beta_X = 0.94 \pm 0.03$  with  $\chi^2 = 127$  for 198 DOF) is obtained when including the absorption and fitting data in the full 0.4–10 keV band (this data has superior photon statistics compared to the 2–10 keV band). We adopt  $\beta_X = 0.94 \pm 0.03$  for the X-ray spectral slope 1.4 days after the burst since this value was derived from the spectrum with the better noise properties.

No extragalactic absorption is required along the line of sight to GRB 021004 and the upper limit on the absorbing column density is  $3.4 \times 10^{21} \text{ cm}^{-2}$ . This result is consistent with the upper limit of  $1.1 \times 10^{20} \text{ cm}^{-2}$  on the H I column density found by Møller et al. (2002). Scaling the value of the fixed Galactic absorption up (down) by a factor of two results in only a 0.03 decrease (increase) in the value of the best-fitting spectral index. We find no evidence for additional spectral features such as lines or absorption edges.

Table 1. Positions and photometry of the secondary standard stars A–G taken from Henden (2002).

| Star | R.A.        | Dec.        | <i>U</i>           | <i>B</i>           | <i>V</i>           | <i>R<sub>C</sub></i> | <i>I<sub>C</sub></i> |
|------|-------------|-------------|--------------------|--------------------|--------------------|----------------------|----------------------|
| A    | 00:27:00.84 | +18:56:38.4 | $20.699 \pm 0.038$ | $19.480 \pm 0.018$ | $17.989 \pm 0.016$ | $17.058 \pm 0.023$   | $16.084 \pm 0.051$   |
| B    | 00:26:57.89 | +18:56:06.7 | $17.372 \pm 0.027$ | $17.341 \pm 0.026$ | $16.699 \pm 0.006$ | $16.333 \pm 0.013$   | $15.948 \pm 0.025$   |
| C    | 00:26:53.61 | +18:56:22.6 | ...                | $21.116 \pm 0.11$  | $19.741 \pm 0.037$ | $18.785 \pm 0.057$   | $17.828 \pm 0.065$   |
| D    | 00:26:52.36 | +18:56:39.5 | ...                | $19.765 \pm 0.032$ | $18.287 \pm 0.018$ | $17.364 \pm 0.028$   | $16.455 \pm 0.033$   |
| E    | 00:26:51.42 | +18:54:36.0 | $18.099 \pm 0.021$ | $18.091 \pm 0.013$ | $17.493 \pm 0.009$ | $17.142 \pm 0.013$   | $16.787 \pm 0.027$   |
| F    | 00:26:58.77 | +18:56:56.0 | $18.545 \pm 0.044$ | $17.430 \pm 0.029$ | $16.258 \pm 0.006$ | $15.538 \pm 0.016$   | $14.896 \pm 0.028$   |
| G    | 00:27:00.56 | +18:54:14.8 | $17.616 \pm 0.060$ | $17.836 \pm 0.033$ | $17.323 \pm 0.006$ | $17.002 \pm 0.008$   | $16.643 \pm 0.015$   |

Table 2. Log of the GRB 021004 observations and the results of the photometry. The UT date is the middle of each exposure.

| UT Date                           | Magnitude    | Seeing (") | $t$ (s) | UT Date                                 | Magnitude    | Seeing (") | $t$ (s) |
|-----------------------------------|--------------|------------|---------|---|--------------|------------|---------|
| <b><i>U</i>-band:</b>             |              |            |         | <b><i>R<sub>C</sub></i>-band cont.:</b> |              |            |         |
| Oct. 6.8880                       | 20.88 ± 0.02 | 1.3        | 1000    | 6.0092                                  | 19.76 ± 0.03 | 1.2        | 300     |
| 7.8880                            | 21.18 ± 0.02 | 1.9        | 1000    | 6.1221                                  | 19.91 ± 0.03 | 1.6        | 600     |
| 8.8880                            | 21.52 ± 0.03 | 1.7        | 1000    | 6.1733                                  | 19.94 ± 0.03 | 1.4        | 600     |
| 10.0925                           | 21.92 ± 0.12 | 1.8        | 900     | 6.2085                                  | 19.92 ± 0.03 | 1.6        | 600     |
|                                   |              |            |         | 6.8348                                  | 20.03 ± 0.03 | 1.4        | 600     |
|                                   |              |            |         | 6.8633                                  | 20.10 ± 0.03 | 1.3        | 600     |
| <b><i>B</i>-band:</b>             |              |            |         |   |              |            |         |
| Oct. 5.9441                       | 20.71 ± 0.02 | 1.0        | 600     | 6.9175                                  | 20.13 ± 0.03 | 1.2        | 600     |
| 10.0639                           | 22.15 ± 0.05 | 1.8        | 600     | 6.9255                                  | 20.12 ± 0.03 | 1.2        | 600     |
|                                   |              |            |         | 7.0391                                  | 20.16 ± 0.03 | 1.0        | 600     |
| <b><i>V</i>-band:</b>             |              |            |         |   |              |            |         |
| Oct. 10.0710                      | 21.49 ± 0.09 | 1.8        | 300     | 7.8451                                  | 20.40 ± 0.03 | 1.5        | 600     |
|                                   |              |            |         | 7.8531                                  | 20.40 ± 0.03 | 1.5        | 600     |
|                                   |              |            |         | 7.8925                                  | 20.43 ± 0.03 | 1.5        | 600     |
| <b><i>R<sub>C</sub></i>-band:</b> |              |            |         |   |              |            |         |
| Oct. 4.8472                       | 18.02 ± 0.03 | 1.5        | 300     | 7.9479                                  | 20.42 ± 0.03 | 1.5        | 600     |
| 4.8517                            | 18.04 ± 0.03 | 1.5        | 300     | 8.0151                                  | 20.43 ± 0.03 | 1.2        | 600     |
| 4.9103                            | 18.23 ± 0.03 | 1.6        | 300     | 8.1412                                  | 20.49 ± 0.03 | 1.2        | 600     |
| 4.9445                            | 18.32 ± 0.03 | 1.8        | 300     | 8.8514                                  | 20.70 ± 0.03 | 1.5        | 600     |
| 4.9987                            | 18.60 ± 0.03 | 1.8        | 300     | 8.9249                                  | 20.77 ± 0.03 | 1.4        | 600     |
| 5.0638 <sup>a</sup>               | 18.84 ± 0.02 | 3.6        | 300     | 9.0047                                  | 20.81 ± 0.03 | 1.1        | 600     |
| 5.0687 <sup>a</sup>               | 18.86 ± 0.03 | 3.3        | 300     | 9.0726                                  | 20.83 ± 0.02 | 1.5        | 600     |
| 5.1193 <sup>a</sup>               | 18.98 ± 0.02 | 3.7        | 500     | 9.1434                                  | 20.85 ± 0.03 | 1.3        | 600     |
| 5.1264 <sup>a</sup>               | 18.98 ± 0.02 | 3.3        | 500     | 10.0759                                 | 21.05 ± 0.02 | 1.5        | 300     |
| 5.1332 <sup>a</sup>               | 19.01 ± 0.02 | 4.1        | 500     | 10.1022                                 | 21.08 ± 0.02 | 1.5        | 6480    |
| 5.1402 <sup>a</sup>               | 19.02 ± 0.03 | 3.7        | 500     | 14.0431                                 | 21.90 ± 0.02 | 0.8        | 600     |
| 5.1470 <sup>a</sup>               | 19.06 ± 0.02 | 3.6        | 500     | 14.0518                                 | 21.95 ± 0.03 | 0.9        | 600     |
| 5.1541 <sup>a</sup>               | 19.08 ± 0.03 | 4.0        | 500     | 14.0600                                 | 21.93 ± 0.03 | 0.9        | 600     |
| 5.1609 <sup>a</sup>               | 19.09 ± 0.02 | 4.0        | 500     | 19.0622 <sup>b</sup>                    | 22.70 ± 0.16 | 1.1        | 1800    |
| 5.1678 <sup>a</sup>               | 19.13 ± 0.02 | 4.7        | 500     | 27.9970                                 | 23.22 ± 0.08 | 1.0        | 3600    |
| 5.1746 <sup>a</sup>               | 19.11 ± 0.02 | 5.1        | 500     | Nov. 4.0158 <sup>b</sup>                | 23.54 ± 0.11 | 1.0        | 7200    |
| 5.1802 <sup>a</sup>               | 19.11 ± 0.02 | 4.7        | 300     |   |              |            |         |
| 5.1860 <sup>a</sup>               | 19.13 ± 0.02 | 3.7        | 500     | <b><i>I<sub>C</sub></i>-band:</b>       |              |            |         |
| 5.1929 <sup>a</sup>               | 19.14 ± 0.03 | 3.8        | 500     | Oct. 4.8563                             | 17.55 ± 0.02 | 1.3        | 300     |
| 5.8541                            | 19.61 ± 0.03 | 2.0        | 600     | 7.8851                                  | 19.92 ± 0.02 | 1.2        | 500     |
| 5.8621                            | 19.62 ± 0.03 | 1.7        | 600     | 8.8851                                  | 20.27 ± 0.02 | 1.5        | 500     |
| 5.9358                            | 19.69 ± 0.03 | 1.8        | 600     | 10.0828                                 | 20.49 ± 0.01 | 1.3        | 600     |

<sup>a</sup>The image was rebinned  $2 \times 2$  to improve the signal-to-noise ratio.

<sup>b</sup>The image was obtained with MOSCA.

### 3. Results

#### 3.1. The Slope of the Optical Spectrum

We used our  $UBVR_CI_C$  photometry from Oct. 10 and the near-simultaneous  $H$ -band photometry of Stefanon et al. (2002) to construct the spectral energy distribution (SED) of the OA 5.568 days after the burst. The optical magnitudes were rescaled to the epoch of the  $H$ -band measurement (Oct. 10.072 UT) and converted to flux densities based on Fukugita et al. (1995).  $H$ -band magnitude–flux density conversion factor was taken from Allen (2000). Finally, the photometric points were corrected for Galactic reddening.

The SED was fit by  $f_\nu(\nu) \propto \nu^{-\beta_{UH}} \times 10^{-0.4A(\nu)}$ , where  $f_\nu(\nu)$  is the flux density at frequency  $\nu$ ,  $\beta_{UH}$  is the intrinsic optical spectral index between the  $U$  and  $H$  photometric bands (approximately 3600–16 000 Å), and  $A(\nu)$  is the extra-galactic extinction along the line of sight to the burst. The dependence of  $A(\nu)$  on  $\nu$  has been parameterized in terms of the rest frame  $A_V$  following the three extinction laws given by Pei (1992) for the Milky Way (MW), the Large Magellanic Cloud (LMC), and the Small Magellanic Cloud (SMC). The fit provides  $\beta_{UH}$  and  $A_V$  simultaneously for the assumed extinction laws. For comparison purposes the unextincted case ( $A_V = 0$ ) was also considered.

Fig. 3 shows that  $A_V = 0$  is not consistent with our data ( $\chi^2/\text{DOF} = 12.3$ ). We find the best fit ( $\chi^2/\text{DOF} = 0.49$ ) with an SMC extinction law having  $A_V = 0.26 \pm 0.04$  and  $\beta_{UH} = 0.39 \pm 0.12$ . The MW and LMC extinction laws give unacceptable fits ( $\chi^2/\text{DOF} = 16.4$  and  $\chi^2/\text{DOF} = 3.8$  respectively). This is the shallowest spectral slope seen for any GRB OA. We find no evidence that the slope of the optical SED changed between approximately 0.35 and 5.5 days after the burst. If we fix  $\beta_{UH} = 1$ , so that it is the same as the spectral slope at  $X$ -ray frequencies, then none of the extinction laws give acceptable fits ( $\chi^2/\text{DOF} > 8$ ). This strongly suggests that there is a spectral break between the optical and  $X$ -ray bands at  $t = 1.4$  days.

The red edge of the Ly $\alpha$  forest for a source at  $z = 2.3351$  lies between the  $U$  and  $B$  bands, so our  $U$ -band data could be significantly affected by intergalactic absorption. In order to test this we repeated our fits using only the  $BVR_CI_CH$  photometry. The results are consistent to within  $1\sigma$  of those obtained if the  $U$ -band data is included. Therefore we believe that intergalactic Ly $\alpha$  absorption is not significantly affecting our estimate of the intrinsic spectral slope at optical wavelengths.

Møller et al. (2002) find absorption systems at  $z = 1.38$  and  $1.60$  in addition to those at  $z \approx 2.3$ . We repeated our fits placing the absorbing dust at these lower redshifts and found that the fits were comparable to those for absorption at  $z = 2.3351$ . Therefore, we are not able to constrain the redshift of the dust. The total absorption is  $0.3 \lesssim A_V \lesssim 0.5$  in the rest frame of the dust regardless of redshift of the dust.



### 3.2. The Location of the Cooling Break

We find  $U - R_C = 0.76 \pm 0.02$  between Oct. 6.9 and Oct. 10.1. When Galactic reddening is taken into consideration this color is consistent with the Oct. 7.29 spectrum of Matheson et al. (2003). This suggests that there was no significant spectral evolution in the optical between 2.4 and 5.5 days after the burst. Our photometry also shows no evidence for color evolution redward of approximately 6588 Å between 0.35 and 5.5 days, therefore we believe that  $\beta_{UH} = 0.39 \pm 0.12$  at optical wavelengths between 0.35 and 5.5 days. The lack of color evolution redward of approximately 6588 Å, and the change in the intrinsic spectral slope between the optical and  $X$ -ray bands, suggest that the increase in  $B - V$  seen by Matheson et al. (2003) between 0.76 and 2.75 days after the burst was not due to a spectral break passing through the optical frequencies.

The different values for the optical and  $X$ -ray spectral slopes 1.4 days after the suggests that there is a spectral break between them at this time. We find  $R_C - I_C = 0.53 \pm 0.02$  for  $0.35 < t < 5.5$  days, which suggests that this break did *not* pass through the optical during our observations.

The relationships between  $\beta_{UH}$ , the slope of the optical decay,  $\alpha$ , and the electron index,  $p$ , given by Sari et al. (1999) (for a homogeneous interstellar medium (ISM)) and Chevalier & Li (1999) (for a pre-existing stellar wind) allow us to use  $\beta_{UH}$  and  $\beta_X$  to predict  $p$  and  $\alpha$  during this period. These predictions are listed in Table 3 where  $p_{UH}$  and  $p_X$  are the electron indices predicted from the optical and  $X$ -ray spectral slopes respectively. In cases where  $1 < p < 2$  the relationships of Dai & Cheng (2001) were used. Situations with  $p < 1$  are unphysical and can be ruled out. We can also rule out cases where both the cooling frequency,  $\nu_c$ , and the synchrotron frequency,  $\nu_m$ , are above the optical since they predict a rising spectrum ( $\beta_{UH} < 0$ ) in the optical. Therefore, our results that  $\beta_{UH} = 0.39 \pm 0.12$  and  $\beta_X = 0.94 \pm 0.03$  require that either  $\nu_m < \nu < \nu_c$  or  $\nu_c < \nu < \nu_m$ .

Fig. 4 shows all of our NOT data for GRB 021004 while Fig. 5 shows our NOT  $R_C$ -band data, and the  $R_C$ -band data from the GCN Circulars up to GCN 1717 (2002 Dec. 2, Fatkhullin et al. (2002)). The NOT data constrain the decay slope to be  $0.75 \lesssim \alpha \lesssim 1.00$ , so we can rule out  $\nu_c < \nu < \nu_m$ , which predicts  $\alpha = 0.25$ . Therefore, we suggest that  $\nu_m < \nu < \nu_c$  during this period and that the electrons were in the slow cooling regime. This implies that the cooling frequency is between the optical and  $X$ -ray bands between 0.35 and 5.5 days after the burst. Averaging  $p_{UH}$  and  $p_X$  gives  $p = 1.9 \pm 0.1$  (standard error). If the burst occurred in a pre-existing stellar wind then the expected optical decay slope after the cooling break is  $\alpha = 1.24$ , which is ruled out by the data. Therefore, we believe that the burst occurred in an ambient medium that was homogeneous over large scales and that the cooling frequency is decreasing with time. In this scenario the predicted optical decay slope is 0.73 before the cooling break passes through the optical and 0.98 after. Fig. 5 shows all of the available  $R_C$ -band data for GRB 021004 with an optical decay of 0.73 for  $t \leq 5$  days after the burst.

### 3.3. The Optical Light Curve

To search for a break in the optical decay we fit the NOT  $R_C$ -band data with a broken power law of the form

$$R_{C,\text{fit}}(t) = \begin{cases} -48.77 - 2.5 \log_{10} (f_\nu(t_b)(t/t_b)^{-\alpha_1}), & \text{if } t \leq t_b \\ -48.77 - 2.5 \log_{10} (f_\nu(t_b)(t/t_b)^{-\alpha_2}), & \text{if } t > t_b \end{cases}. \quad (1)$$

where  $t_b$  is the time of the break in the power law,  $f_\nu(t_b)$  is the flux in the  $R_C$  band at the time of the break,  $f_{\text{host}}$  is the  $R_C$ -band flux from the host galaxy, and  $\alpha_1, \alpha_2$  are the decay slopes before and after the break respectively. This formalism makes no assumptions about the physical causes of the break. The best fit occurs with  $\alpha_1 = 0.85^{+0.01}_{-0.01}$ ,  $\alpha_2 = 1.43^{+0.03}_{-0.03}$ ,  $t_b = 4.74^{+0.14}_{-0.80}$  days, and  $f_\nu(t_b) = 14.675^{+3.209}_{-0.445} \mu\text{Jy}$  which corresponds to  $R_C(t_b) = 20.81 \pm 0.03$ . This fit is shown in Fig. 4. The large formal errors in the break time indicate that the break was probably gradual and occurred over a period of approximately one day.

The lack of color evolution between 0.35 and 5.5 days means that the break can not be due to the cooling frequency passing through the optical. In addition, the predicted slope after the cooling break is  $\alpha_2 = 0.98$  whereas we find  $\alpha_2 = 1.43^{+0.03}_{-0.03}$ , which is inconsistent with the expected slope after the cooling break. Therefore, the break at  $t \approx 5$  days is most likely due to the Lorentz factor of the fireball falling below  $1/\theta_j$  where  $\theta_j$  is the half-opening angle of the jet. For a jet that is undergoing sideways expansion the slope of the optical decay after the jet break is  $\alpha_j = (p+6)/4$  (Dai & Cheng 2001), so we expect to see  $\alpha_j = 1.98 \pm 0.03$ .

### 3.4. The Properties of the Jet

We applied cosmological  $K$  corrections (Bloom et al. 2001) and averaged the FREGATE fluences in the 50–300 keV and 7–400 keV bands to correct them to the 20–2000 keV band. The corrected fluences were then averaged to get an isotropic equivalent energy of  $E_{\text{iso}} = (2.2 \pm 0.3) \times 10^{52}$  erg. We estimate the opening angle of the GRB jet using Rhoads (1999) and Sari et al. (1999) and the formalism of Frail et al. (2001). This yields  $\theta_j \approx (5.8 \pm 0.9)(n/0.1)^{1/8}$  if we assume, as did Frail et al. (2001), that the efficiency of converting energy in the ejecta into gamma rays is 0.2. We note that our result is not very sensitive to this efficiency. Reducing the efficiency to 0.01 only changes  $\theta_j$  by approximately 30%. We estimate that GRB 021004’s intrinsic energy in gamma rays, after correcting for the jet geometry, was  $E_\gamma \approx (1.1 \pm 0.2) \times 10^{50}(n/0.1)^{1/4}$  erg. This is only approximately  $2\sigma$  smaller than the canonical value of  $(5 \pm 2) \times 10^{50}$  erg (Frail et al. 2001; Piran et al. 2001; Panaitescu & Kumar 2002).

In order for this burst to have had the “standard” energy the ambient density must be  $n \approx 35 \text{ cm}^{-3}$ . This is in agreement with the particle densities ( $0.1 < n < 100 \text{ cm}^{-3}$ ) found by Panaitescu & Kumar (2001) for ten GRBs. It is also similar to the densities found in some supernova remnants.

Cox et al. (1999) and Shelton et al. (1999) find a mean density of  $6 \text{ cm}^{-3}$  with large density gradients for the supernova remnant W44 while Achterberg & Ball (1994) find  $n \approx 125 \text{ cm}^{-3}$  approximately one pc from the progenitor of SN1978K. Lazzati et al. (2002) and Nakar et al. (2002) find that the observed variations in the optical decay of GRB 021004 are consistent with density variations of  $\Delta n/n \approx 10$  within approximately  $10^{17}$ – $10^{18}$  cm of the progenitor. Therefore, we believe that GRB 021004 occurred in an environment with a mean density that is typical of other GRBs.

#### 4. Discussion

Our NOT photometry, when combined with the *Chandra* X-ray spectrum, suggests that the electron index for GRB 021004 is  $p = 1.9 \pm 0.1$ . Most GRBs are well fit by models with  $p \approx 2.3$ – $2.5$  (van Paradijs et al. 2000). Panaitescu & Kumar (2002) present models for ten GRBs and find that five are best fit with  $p < 2$ . The mean electron index for the ten bursts in their study is  $\bar{p} = 1.9$ . Electron indices of less than two represent infinite energy in the standard relativistic fireball model (Mészáros 2002). This can be avoided by introducing an upper limit for the electron energy distribution (Dai & Cheng 2001), but detailed modeling of the acceleration of particles in highly relativistic shocks predict that the electron index should be approximately 2.3 (Achterberg et al. 2001), which is inconsistent with our results. The fact that many GRBs appear to have electron indices of less than two may indicate the need for detailed hydrodynamic modeling of GRB afterglows in order to accurately determine the fireball parameters.

Our results are consistent with a clumpy ISM near the progenitor as proposed by Lazzati et al. (2002). Their scenario assumes that the GRB occurred in an ISM that is inhomogeneous on sub-parsec scales and predicts  $p \approx 2$ . Variations in the density of the ambient medium of  $\Delta n/n \approx 10$  can explain the observed fluctuations on the optical decay of GRB 021004. Nakar et al. (2002) have shown that the deviations from a power law in the optical decay can be used to reconstruct the density profile in the vicinity of the progenitor. Both groups find that the observed variations in the optical decay of GRB 021004 are consistent with an ambient medium that is homogeneous on scales of approximately  $10^{18}$  cm with a density enhancement of  $\Delta n/n \approx 10$  at approximately  $10^{17}$  cm from the progenitor. The observations of GRB 021004 are also broadly consistent with a relativistic fireball crossing a discontinuity in the ISM. Dai & Lu (2002) find that a density jump at  $R \approx 10^{17}$  cm from a GRB can produce an increase of a factor of a few in the optical flux.

Extrapolating the predicted pre-cooling break slope to approximately ten minutes after the burst (see Fig. 5) shows that the early data of Fox (2002) are consistent with our predicted optical decay of  $\alpha = 0.73$  before the cooling break. Kobayashi & Zhang (2003) present a model where the optical flux before approximately one hour after the burst is dominated by optical emission from reverse shocks. Their model requires  $p \approx 2.4$ , which is significantly higher than the electron index which we deduce from the X-ray and optical spectra. The agreement between the optical decay which is predicted by the spectral slopes and that seen at approximately ten minutes after the burst suggests that the physical mechanism controlling the observed flux at  $t \approx 10$  minutes is

the same as the one operating at  $t > 0.5$  days.

## 5. Conclusions

We present  $UBVR_CI_C$  photometry of the OA of GRB 021004 taken at the NOT and *Chandra* X-ray data. The optical data were taken between approximately eight hours and 30 days after the burst while the X-ray data was taken approximately one day after the burst. The broad-band optical SED yields an intrinsic spectral slope of  $\beta_{UH} = 0.39 \pm 0.12$  while the X-ray data gives  $\beta_X = 0.94 \pm 0.03$ . There is no evidence for color evolution between 8.5 hours and 5.5 days after the burst. We find an extragalactic extinction of  $0.3 \lesssim A_V \lesssim 0.5$  along the line of sight to the burst. Our data suggest that this dust has an SMC extinction law but we are not able to constrain its redshift.

The spectral slopes have been combined with the observed  $R_C$ -band optical decay to determine that the shocked electrons are in the slow cooling regime with an electron index of  $1.9 \pm 0.1$ , and that the burst occurred in an ISM that is homogeneous on scales larger than approximately  $10^{18}$  cm. Our data are consistent with an optical decay of  $\alpha = 0.73$  at  $t \lesssim 5$  days after the burst, and  $\alpha = 1.98$  after that. There is evidence that the transition between the early and late decay slopes occurred over a period of approximately one day. This is consistent with a sideways expanding jet that slows to a Lorentz factor of  $\Gamma \approx 10$  approximately six days after the burst. The total gamma-ray energy in the burst was  $E_\gamma = (1.1 \pm 0.2) \times 10^{50} (n/0.1)^{1/4}$  erg. The ambient density around GRB 021004 is consistent with what is seen around other GRBs ( $0.1 < n < 100 \text{ cm}^{-3}$ ) and with densities seen in supernova remnants (Achterberg & Ball 1994; Cox et al. 1999; Shelton et al. 1999).

The rapid localization of GRB 021004 and the near-continuous monitoring of its OA from approximately ten minutes after the burst occurred has allowed this burst to be studied in unprecedented detail. The afterglow shows a large increase in luminosity approximately 2.5 hours after the burst and a possible second, smaller increase at  $t \approx 1$  day. Both of these features would have been missed if optical follow-up had not been immediate and continuous. Further, if the OA had not been identified until more than approximately three hours after the burst the true nature of the early-time slope would not have been known. GRB 021004 demonstrates the need for continuous early-time monitoring of GRB OAs.

We wish to thank the *HETE-II* team, Scott Barthelmy, and the GRB Coordinates Network (GCN) for rapidly providing precise GRB positions to the astronomical community. We also wish to thank Arne Henden for providing precision photometry of stars in the field of GRB 021004. STH acknowledges support from the NASA LTSA grant NAG5-9364. JPUF gratefully acknowledges support from the Carlsberg Foundation. JG acknowledges the receipt of a Marie Curie Research Grant from the European Commission. JMCC acknowledges the receipt of an FPI doctoral fellow-

ship from Spain's Ministerio de Ciencia y Tecnología. Several of the authors would like to thank the University of Copenhagen for its hospitality while this paper was being prepared. This research has made use of the NASA/IPAC Extragalactic Database (NED), which is operated by the Jet Propulsion Laboratory, California Institute of Technology, under contract with NASA. This paper includes the first data obtained with MOSCA, which is funded by the Carlsberg Foundation. This work is supported by the Danish Natural Science Research Council (SNF).

## REFERENCES

- Achterberg, A., Gallant, Y. A., Kirk, J. G., & Guthmann, A. W. 2001, *MNRAS*, 328, 393
- Achterberg, A., & Ball, L. 1994, *A&A*, 285, 687
- Allen, C. W. 2000, *Astrophysical Quantities*, 4<sup>th</sup> edition, 2000, ed. A. N. Cox.
- Bloom, J. S., Frail, D. A., & Sari, R. 2001, *AJ*, 121, 2879
- Castro-Tirado, A. J., Gorosabel, J., Benítez, N., et al. 1998, *Science*, 279, 1011
- Chevalier, R. A., & Li, Z.-Y. 1999, *ApJ*, 520, L29
- Chernock, R., & Filippenko, A. V. 2002, *GCNC* 1605
- Cox, D. P., Shelton, R. L., Maciejewski, W., Smith, R. K., Plewa, T., Pawl, A., & Rózycka, M. 1999, *ApJ*, 524, 179
- Dai, L. Z., & Lu, T. 2002, *ApJ*, 565, L87
- Dai, Z. G., & Cheng, K. S. 2001, *ApJ*, 558, L109
- Dickey, J. M., & Lockman, F. J. 1990, *ARA&A*, 28, 215
- Fatkhullin, T. A., Komarova, V. N., Moiseev, A. V. 2002, *GCNC* 1717
- Fox, D. W. 2002, *GCNC* 1564
- Fox, D. W., Barth, A. J., Soderberg, A. M., Price, P. A., Buttery, H., & Mauch, T. 2002, *GCNC* 1569
- Frail, D. A., Kulkarni, S. R., Sari, R., Djorgovski, S. G., Bloom, J. S., Galama, T. J., Reichart, D. E., Dergner, E., et al. 2001, *ApJ*, 562, L55
- Fukugita, M., Shimasaku, K., & Ichikawa, T. 1995, *PASP*, 107, 945
- Garnavich, P. M., Loeb, A., & Stanek, K. Z. 2000, *ApJ*, 544, L11
- Henden, A. 2002, *GCNC* 1630

- Holland, S. T., Soszyński, I., Gladders, M. D., Barrientos, L. F., Berlind, P., Bersier, D., Garnavich, P. M., Jha, S., & Stanek, K. Z. 2002, *AJ*, 124, 639
- Jakobsson, P., Hjorth, J., Fynbo, J. P. U., et al. 2003, *A&A*, submitted
- Kobayashi, S., & Zhang, B. 2003, *ApJ*, 582, L75
- Kouveliotou, C., Meegan, C. A., Fishman, G. J., Bhat, N. P., Briggs, M. S., Koshut, T. M., Paciesas, W. S., & Pendleton, G. N. 1993, *ApJ*, 413, L101
- Lamb, D., Ricker, G., Atteia, J.-L., Kawai, N., Woosley, S. Olive, J.-F., Boer, M., Dezalay, J.-P., Hurley, K., et al. 2002, GCNC 1600
- Lazzati, D., Rossi, E., Covino, S., Ghisellini, G., & Malesani, D. 2002, *A&A*, 396, L5
- Matheson, T., Garnavich, P. M., Foltz, C., West, S., Williams, G., Falco, E., Calkins, M. L., Castander, F. J., et al. 2003, *ApJ*, 582, L5
- Mészáros, P. 2002 *ARA&A*, 40, 137
- Møller, P., Fynbo, J. P. U., Hjorth, J., Thomsen, B., Egholm, M. P., Andersen, M. I., Gorosabel, J., Holland, S. T., et al. 2002, *A&A*, 396, L21
- Nakar, E., Piran, T., & Granot, J. 2002, *New Astronomy*, submitted, astro-ph/0210631
- Panaiteescu, A., & Kumar, P. 2001, *ApJ*, 554, 667
- Panaiteescu, A., & Kumar, P. 2002, *ApJ*, 571, 779
- Panaiteescu, A., Mészáros, P., & Rees, M. J. 1998, *ApJ*, 503, 314
- Pedersen, H., Jaunsen, A. O., Grav, T., et al. 1998, *ApJ*, 496, 311
- Pei, Y. C. 1992, *ApJ*, 395, L30
- Piran, T., Kumar, P., Panaiteescu, A., & Piro, L. 2001, *ApJ*, 560, L167
- Rhoads, J. E. 1999, *ApJ*, 525, 737
- Sahu, D. K., Bhatt, B. C., Anupama, G. C., & Prabhu, T. P. 2002, GCNC 1587
- Sako, M., & Harrison, F. 2002, GCNC 1624
- Salamanca, I., Rol, E., Wijers, R., Ellison, S., Kaper, L., Tanvir, N. 2002, GCNC 1611
- Sari, R., Piran, T., & Halpern, J. P. 1999, *ApJ*, 519, L17
- Savaglio, S., Fiore, F., Israel, G., Marconi, G., Antonelli, L. A., Fontana, A., Stella, L., Di Paola, A., et al. 2002, GCNC 1633

- Schlegel, D. J., Finkbeiner, D. P., & Davis, M. 1998, *ApJ*, 500, 525
- Shelton, R. L., Cox, D. P., Maciejewski, W., Smith, R. K., Plewa, T., Pawl, A., Rózyńska, M. 1999, *ApJ*, 524, 192
- Shirasaki, Y., Graziani, C., Matsuoka, M., Tamagawa, T., Torii, K., Sakamoto, T., Yoshida, A., Fenimore, E., et al. 2002, GCNC 1565
- Stefanon, M., Covino, S., Malesani, D., Ghisellini, G., Fugazza, D., Tescini, G., Masetti, N., & Pian, E. 2002, GCNC 1623
- Stetson, P. B. 1987, *PASP*, 99, 191
- Stetson, P. B., & Harris, W. E. 1988, *AJ*, 96, 909
- Torii, K., Kato, T., & Yamaoka, H. 2002, GCNC 1589
- van Paradijs, J., Kouveliotou, C., & Wijers, R. A. M. J. 2000, *ARA&A*, 38, 379
- Winn, J., Bersier, D., Stanek, K. Z., Garnavich, P. M., & Walker, A. 2002, GCNC 1576

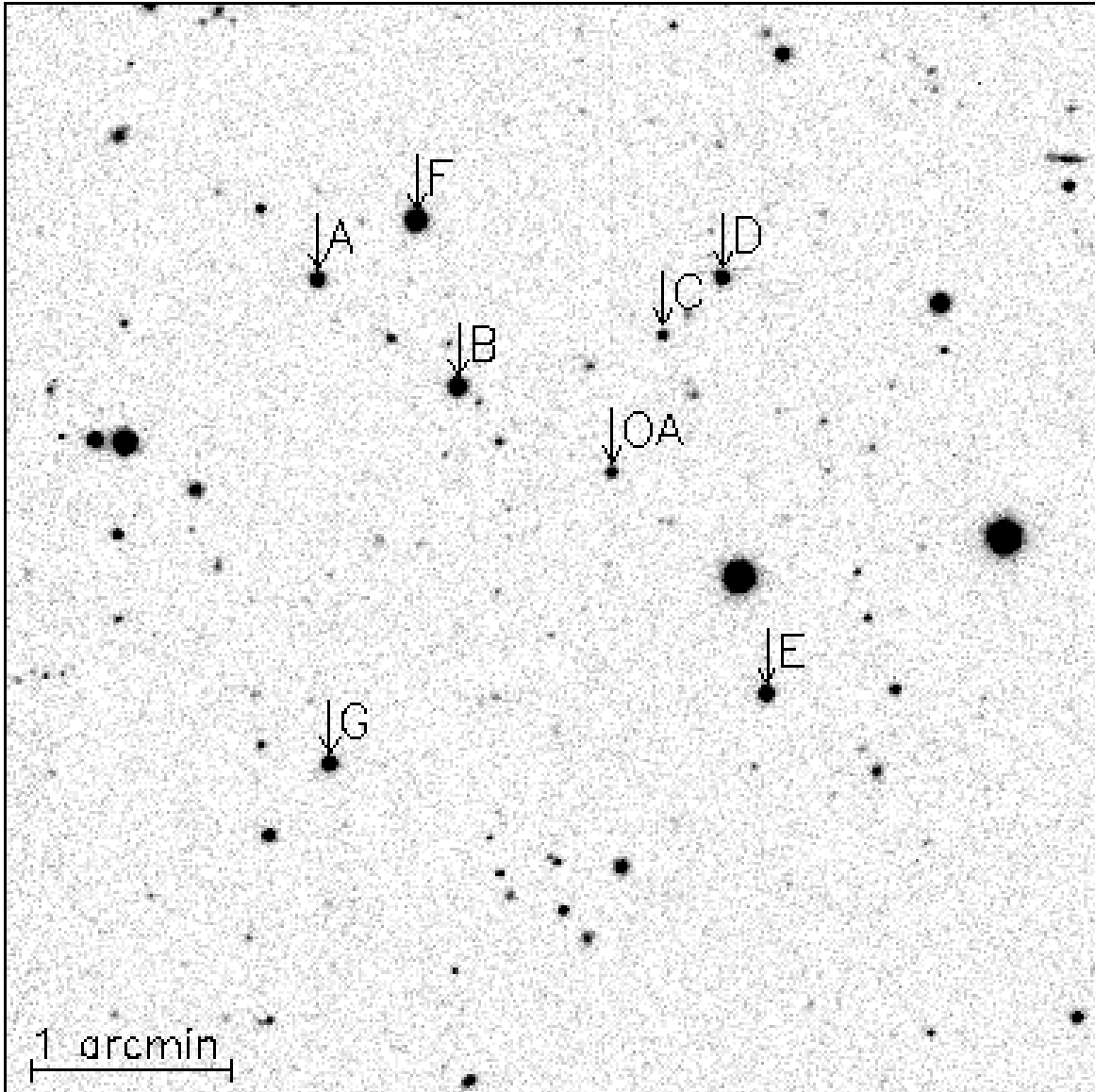


Fig. 1.— The field of GRB 021004 in the  $R_C$  band. The stars marked A–G are used as secondary standards for the relative photometry. The positions and photometry of these secondary standard stars are given in Table 1. North is up and east is to the left. The OA is isolated so there is no confusion with neighbouring sources.



Chandra HEG/MEG -1/+1 orders + zero'th order

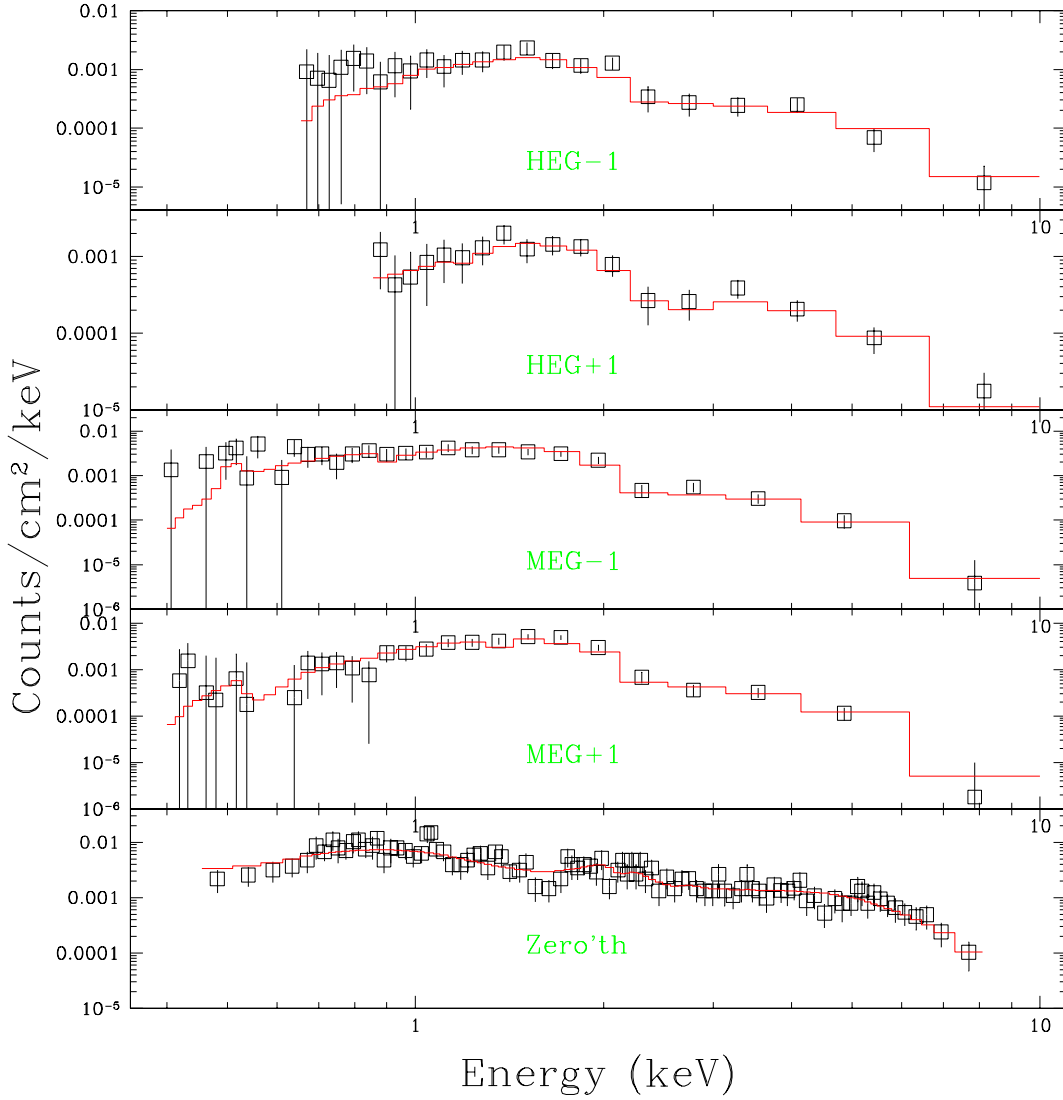


Fig. 2.— First order *Chandra* High Energy Grating/Medium Energy Grating spectra and zero'th order spectrum of GRB 021004 with the best fit model jointly fit to all spectra. The lines show an intrinsic power law with no absorption in the vicinity of GRB 021004 (at  $z = 2.3351$ ) and a fixed Galactic absorption of  $N(\text{H}) = 1.23 \times 10^{20} \text{ cm}^{-2}$ .

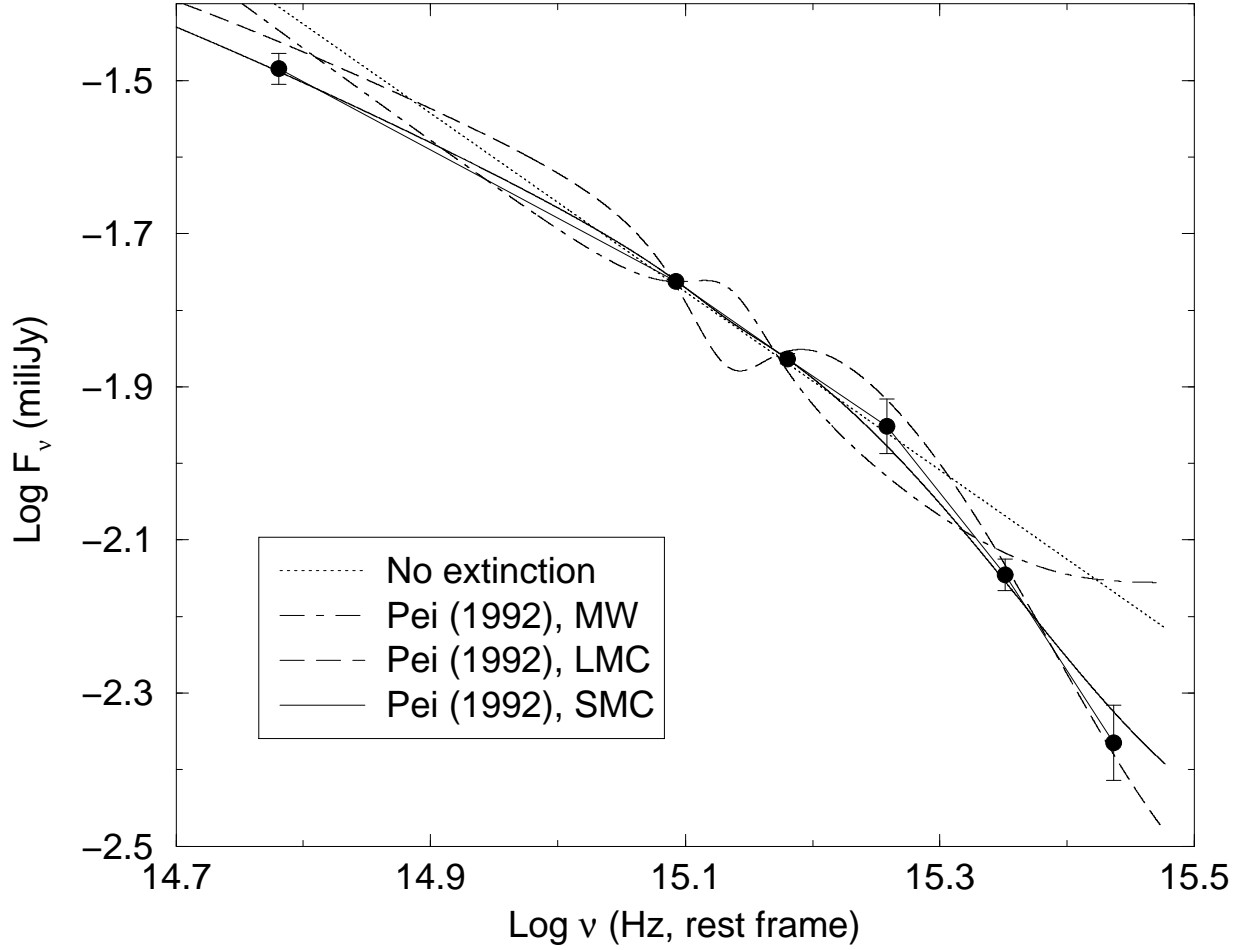


Fig. 3.— The SED of the OA of GRB 021004 on 2002 Oct. 10.072 UT. The filled circles represent our NOT  $UBVR_CI_C$  data and the  $H$ -band data point from Stefanon et al. (2002). In the  $R_C$  and  $I_C$  bands the error bars are smaller than the circles. The lines represent the SED fits when the SMC (solid), LMC (dashed) and MW (dot-dashed) extinction laws given by Pei (1992) are applied. A fit (dotted line) assuming no extinction of the host is shown for comparison. If we assume that the unextinguished spectrum follows  $f_\nu(\nu) \propto \nu^{-\beta}$  then only the SMC extinction provides an acceptable fit to the data points.

Table 3. Predicted electron indices and decay slopes assuming  $\beta_{UH} = 0.39 \pm 0.12$  and  $\beta_X = 0.94 \pm 0.03$ . The predicted early-time slope of the optical decay is denoted  $\alpha$ .

| Model                 | Environment | $p_{UH}$      | $p_X$         | $\alpha$        | Comments                            |
|-----------------------|-------------|---------------|---------------|-----------------|-------------------------------------|
| $\nu_m < \nu_c < \nu$ | ISM         | $0.8 \pm 0.2$ | $1.9 \pm 0.1$ | ...             | $p_{UH}$ and $p_X$ are inconsistent |
|                       | Wind        |               |               | ...             | $p_{UH}$ and $p_X$ are inconsistent |
| $\nu_m < \nu < \nu_c$ | ISM         | $1.8 \pm 0.2$ | $1.9 \pm 0.1$ | $0.73 \pm 0.02$ |                                     |
|                       | Wind        |               |               | $1.24 \pm 0.01$ | $\alpha$ does not fit data          |
| $\nu < \nu_m < \nu_c$ | ISM         | ...           | 1.9 or 2.9    | ...             | Rising spectrum                     |
|                       | Wind        | ...           |               | ...             | Rising spectrum                     |
| $\nu_c < \nu_m < \nu$ | ISM         | $0.8 \pm 0.2$ | $1.9 \pm 0.1$ | ...             | $p_{UH}$ and $p_X$ are inconsistent |
|                       | Wind        |               |               | ...             | $p_{UH}$ and $p_X$ are inconsistent |
| $\nu_c < \nu < \nu_m$ | ISM         | ...           | $1.9 \pm 0.1$ | 1/4             | $\alpha$ does not fit data          |
|                       | Wind        | ...           |               | 1/4             | $\alpha$ does not fit data          |
| $\nu < \nu_c < \nu_m$ | ISM         | ...           | $1.9 \pm 0.1$ | ...             | Rising spectrum                     |
|                       | Wind        | ...           |               | ...             | Rising spectrum                     |

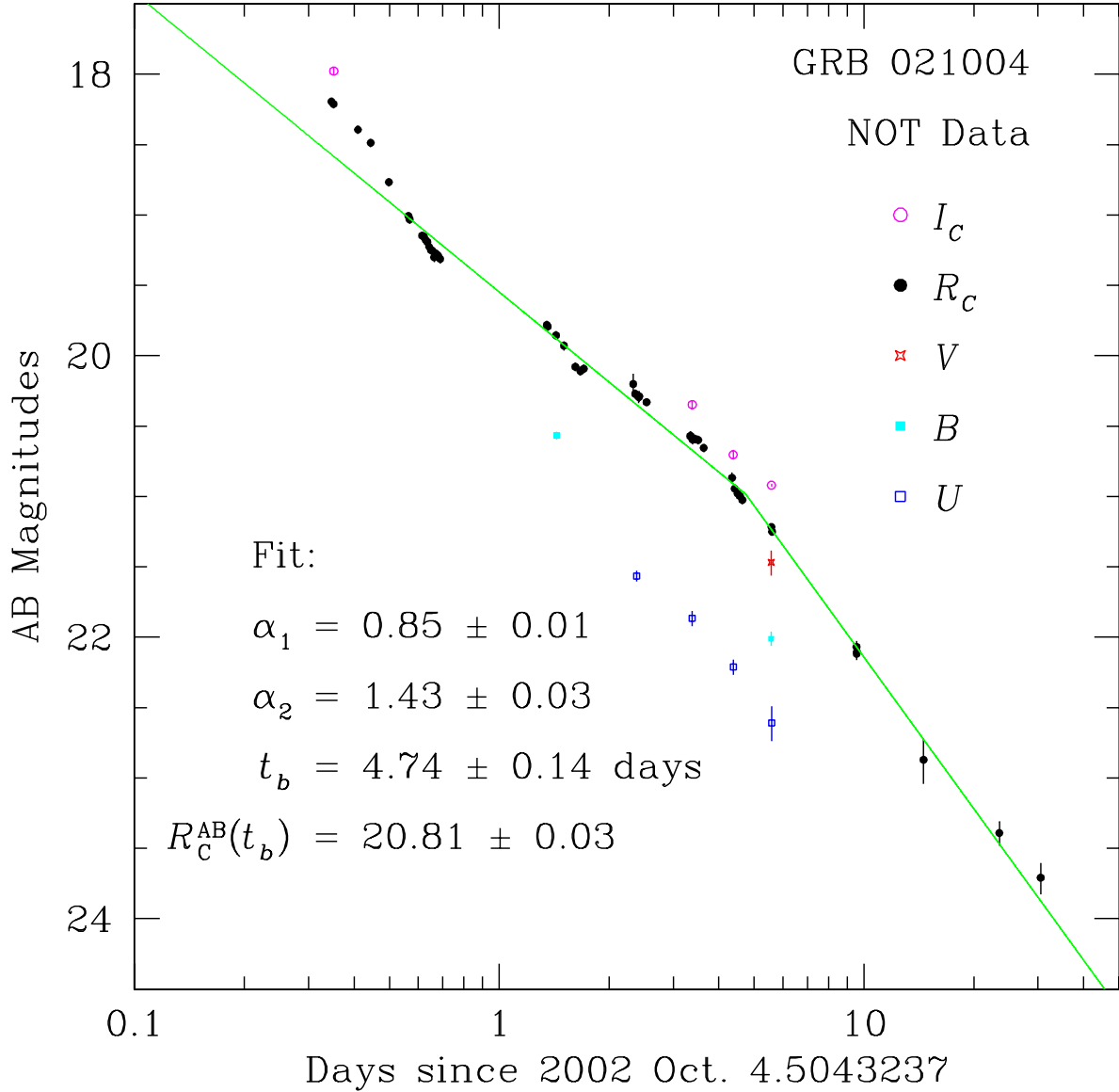


Fig. 4.— This is our NOT data for GRB 021004. The open squares represent the  $U$  band, the closed squares represent the  $B$  band, the stars represent the  $V$  band, the closed circles represent the  $R_C$  band, and the open circles represent the  $I_C$  band. The line is the best-fitting broken power law to the  $R_C$ -band data as described in § 3.3. All of the data in this panel have been scaled to AB magnitudes.

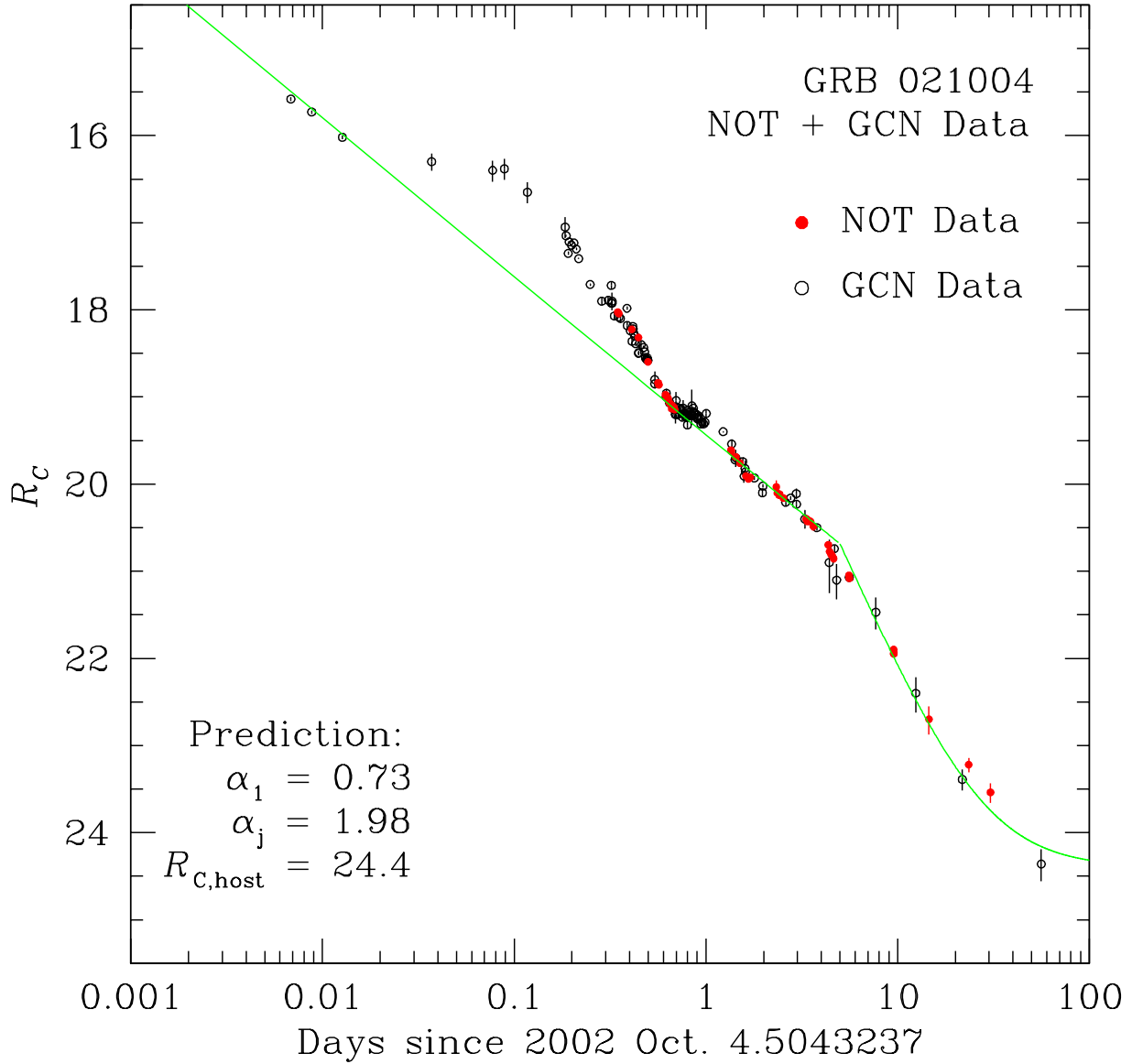


Fig. 5.— This is our NOT  $R_C$ -band data (closed circles) and the  $R_C$ -band data taken from GCN Circulares (open circles) for GRB 021004. The later data have been corrected so that the Fox (2002) comparison star has  $R_C = 15.54 \pm 0.02$  (Henden 2002). The line is the predicted (not fitted)  $R_C$ -band decay with  $p = 2$  in a homogeneous ISM with a host galaxy that is assumed to have  $R_C = 24.4$  (Fatkhullin et al. 2002). The predicted decay flux has been scaled to the NOT data.